

Thermodynamic, spectroscopic and phase equilibrium investigations on polar fluid mixtures at high pressures

Gerhard M. Schneider, Jürgen Ellert, Udo Haarhaus, Ingo F. Hölscher, Gudrun Katzenski-Ohling, Annette Kopner, Jürgen Kulka, Dieter Nickel, Jörg Rübesamen, and Anneliese Wilsch

Physical Chemistry Laboratory, Department of Chemistry, University of Bochum, D-4630 Bochum, Federal Republic of Germany

Abstract - In the present survey some important trends in the high-pressure thermodynamics of fluid mixtures of non-electrolytes are reviewed, the accent being on selected results for polar mixtures that have been recently obtained in our laboratory.

First the pressure dependence of molar excess functions is discussed; it can be obtained from a knowledge of the molar excess volume V_m^E as a function of pressure, temperature, and composition. Results for binary systems consisting of strongly interacting components (e.g. triethylamine + trichloromethane) are presented and attempts are described to determine the hydrogen-bonding parts of the molar excess volume and from these the equilibrium constant K and the standard reaction volume $\Delta_r V^0$ for the formation of the hydrogen bond.

The pressure dependence and critical phenomena of liquid-gas, liquid-liquid, and gas-gas equilibria will be shortly reviewed and some new data will be presented. Here phase separation phenomena in binary as well as ternary systems will be considered, the accent being on solutions of alkanols (e.g. methanol, 1-hexanol, 1-decanol, 1-dodecanol) in liquid (e.g. alkanes) or supercritical (e.g. CO_2 , N_2 , CHF_3 , CClF_3) solvents and their mixtures. For 1-decanol + CO_2 and 1-hexanol + CClF_3 the concentrations of the monomeric and associated alkanol species in the coexisting phases have been determined separately by near-infrared spectroscopy (NIR). Methods for the correlation and calculation of the phase equilibrium data measured are very shortly discussed.

Finally the significance of high-pressure phase equilibria in fluid mixtures for practical applications is briefly described e.g. for fluid extraction and supercritical fluid chromatography (SFC).

INTRODUCTION

It is the aim of the present review to discuss some important trends in the high-pressure thermodynamics of fluid mixtures of non-electrolytes and to demonstrate several interesting and sometimes new effects that often allow a better understanding of the enormous amount of knowledge already obtained at normal pressure. The present written version of the lecture will have an accent on recent, mostly unpublished results on some selected binary and ternary fluid mixtures containing at least one polar component that have been obtained in our laboratory at the University of Bochum during the last two or three years. It will accordingly be a continuation of some older of our review articles in this and related fields (refs 1-6) covering also experimental techniques (ref.7) and kinetic investigations (ref.8). Applications will only briefly be considered; an extensive survey including physico-chemical aspects can be found in three books (refs 9-11) and in the proceedings of several meetings or special issues of some journals; for citations see e.g. refs 5, 9-11.

EXCESS FUNCTIONS OF LIQUID MIXTURES AT HIGH PRESSURES

The pressure dependence of the molar excess Gibbs energy G_m^E , the molar excess entropy S_m^E , and the molar excess enthalpy H_m^E can be obtained from accurate measurements of the molar excess volume V_m^E as a function of temperature T and

pressure p according to the well-known thermodynamic relations:

$$(\partial G_m^E / \partial p)_{T, x} = V_m^E \quad (1)$$

$$(\partial S_m^E / \partial p)_{T, x} = -(\partial V_m^E / \partial T)_{p, x} \quad (2)$$

$$(\partial H_m^E / \partial p)_{T, x} = V_m^E - T \cdot (\partial V_m^E / \partial T)_{p, x} \quad (3)$$

Here V_m^E is defined as

$$V_m^E(T, p, x) \equiv V_m(T, p, x) - \{x_1 \cdot V_{m1}^*(T, p) + x_2 \cdot V_{m2}^*(T, p)\} \quad (4)$$

where $V_m(T, p, x)$ is the molar volume of a mixture of mole fraction x at given temperature and pressure and $V_{m1}^*(T, p)$ and $V_{m2}^*(T, p)$ are the molar volumes of pure components 1 and 2 at given temperature and pressure, respectively. Integration of equations (1) to (3) yields the change of the molar excess functions between atmospheric pressure and the pressure p for a mixture at given temperature and mole fractions. For a more detailed discussion see e.g. ref.4.

In order to evaluate these changes it is necessary to measure the excess volumes as accurately as possible. From measurements at atmospheric pressure it is well-known that direct measurements (where the volume change is observed when two liquids are mixed in a dilatometer) are capable of yielding higher-precision results more readily than the indirect method (when the densities of the pure liquids and their mixtures at known compositions are measured). Our excess-volume measurements were performed according to the direct method in a stainless-steel dilatometer of the batch type, mounted in a high-pressure autoclave. The apparatus has been improved several times and is described in detail elsewhere (ref.12). Accuracies for V_m^E of about $\pm 0.01 \text{ cm}^3 \text{ mol}^{-1}$ are obtained. With this apparatus V_m^E measurements up to a maximum pressure of about 250 MPa were performed on many aqueous and non-aqueous systems; for references see e.g. refs 12, 4.

Here only one example will be treated in somewhat more detail that is within the special scope of this Conference. Very recently an attempt was made in our laboratory to obtain the hydrogen-bonding part of the excess molar volumes $V_m^E(\text{corr})$ of the mixtures (triethylamine or diethylether) + trichloromethane reported in a preceding paper (refs 13, 14) by subtracting the V_m^E values of the corresponding model systems in which trichloromethane was substituted by 1,1,1-trichloroethane and which are expected not to form hydrogen-bonds. In Fig.1 experimental data on the binary systems triethylamine + trichloromethane (Fig.1a; refs 13, 14) and triethylamine + 1,1,1-trichloroethane (Fig.1b; refs 15,16) are given as a function of pressure for $T = 298.15 \text{ K}$. For both systems all excess volumes are negative and the absolute values decrease with increasing pressure, the absolute values and the pressure dependence of V_m^E being considerably higher in the trichloromethane system.

Over the whole mole fraction range values of $V_m^E(\text{corr})$ were calculated at $p = \text{const}$ and $T = \text{const}$ and fitted to the equation:

$$V_m^E(\text{corr}) / \text{cm}^3 \cdot \text{mol}^{-1} = x(1-x) \{A_1 + A_2(1-2x)^2\} \quad (5)$$

With the parameters A_1 and A_2 obtained from Eq(5) values of $V_m^E(\text{corr})$ in the range $0.2 \leq x \leq 0.8$ were calculated and $x(1-x)/V_m^E(\text{corr})$ was plotted against $V_m^E(\text{corr})$ (refs 15, 16). According to the so-called "chemical theory" this plot is expected to show a linear dependence (see ref.17) with the slope S and the intercept I respectively

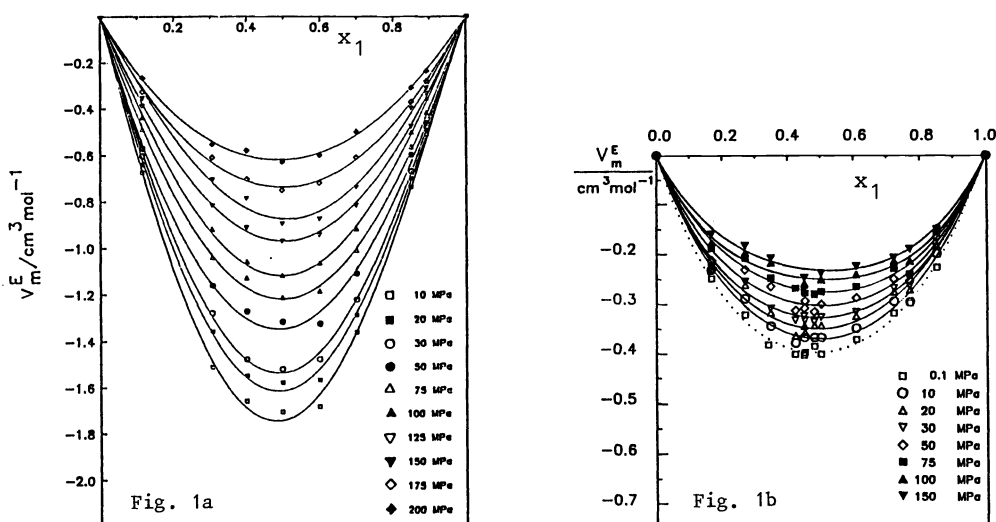
$$S = -(1 + K)/K \Delta_r V^O \quad \text{and} \quad (6)$$

$$I = (1 + K)/K \Delta_r V^O \quad . \quad (7)$$

Combining equations (6) and (7) the standard reaction volume $\Delta_r V^O$ and the equilibrium constant K on mole fraction basis are given by

$$\Delta_r V^O = -I/S \quad \text{and} \quad (8)$$

$$K = -S/(I^2 + S) \quad . \quad (9)$$



a. Triethylamine(2) + chloroform(1)
(Kulka, refs 13, 14)

b. Triethylamine(1) + 1,1,1-trichloroethane(2)
(Rübesamen, refs 15,16)

Fig. 1. Molar excess volumes V_m^E as a function of mole fraction x of binary triethylamine systems at 298.15 K and different pressures

According to the procedure described above these values should correspond to purely hydrogen-bonding properties. The \underline{K} -values determined at low pressures agree reasonably well with data such as obtained from excess enthalpy studies at normal pressure also using the corresponding 1,1,1-trichloroethane mixture as model system (ref.18). The results give evidence for a strong pressure dependence of the \underline{K} and $\Delta_r V^O$ values. For triethylamine + trichloromethane at different pressures and at $\underline{T} = 308.15$ K the \underline{K} and $\Delta_r V^O$ values such as obtained from the plots in Fig.2 are compiled in Table 1. For the isotherm at 298.15 K and the results in the system diethylether + trichloromethane the deviations from the simple chemical theory used were more important. For additional data and details see refs 13-17. More investigations will be necessary to make sure whether the pressure effects such as shown in Table 1 are true or produced by the simplifications of the theory used.

TABLE 1. \underline{K} and $\Delta_r V^O$ values for 308.15 K according to equations (8) and (9) such as obtained from the plot: $(1-x) \cdot x / V_m^E(\text{corr})$ against $V_m^E(\text{corr})$ where $V_m^E(\text{corr}) \equiv \{V_m^E((1-x)(C_2H_5)_3N + xCHCl_3) - V_m^E((1-x)(C_2H_5)_3N + xCH_3CCl_3)\}$ (see Fig.2)

$\frac{p}{\text{MPa}}$	0.1	10	20	30	50	75	100	150
\underline{K}	0.9	0.8	1.5	1.3	2.2	2.1	2.8	3.9
$\frac{\Delta_r V^O}{\text{cm}^3 \cdot \text{mol}^{-1}}$	-11	-12	-8.4	-8.5	-6.2	-5.0	-4.8	-3.7

From the V_m^E values the molar excess Gibbs energy G_m^E can be calculated as a function of pressure by straightforward integration of Eq(1). This has been done for essentially all systems where V_m^E has been measured up to now; for references see e.g. refs 4, 12-16. As an example in Fig.3 $\Delta G_m^E \equiv G_m^E(p) - G_m^E(0.1 \text{ MPa})$ for $x = \text{const}$ and $\underline{T} = \text{const}$ is plotted against pressure p for the system triethylamine + trichloromethane at 298.15 K (refs 13, 14). Since G_m^E is negative for this system and ΔG_m^E is found to be negative, too, G_m^E becomes even more negative with increasing pressure; thus at higher pressures the mixture becomes less ideal with respect to G_m^E and more ideal with respect to V_m^E . Such a situation is by no means unusual and has also been found in other systems (see e.g. ref.4).

It should be mentioned that H_m^E can be determined as a function of pressure by integration of Eq(3). These data can be compared with H_m^E values measured directly in a high-pressure flow calorimeter. This technique has been developed by Christensen et al (e.g. ref.19) and Heintz and Lichtenthaler (e.g. ref.20) and will be of increasing importance in the future.

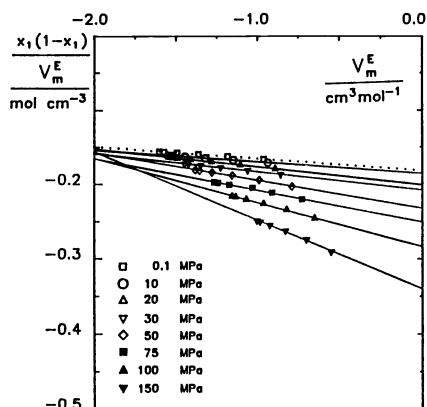


Fig. 2. Determination of K and ΔV^O for triethylamine(1) + Chloroform (2) (Rübesamen, refs 15, 16; see text)

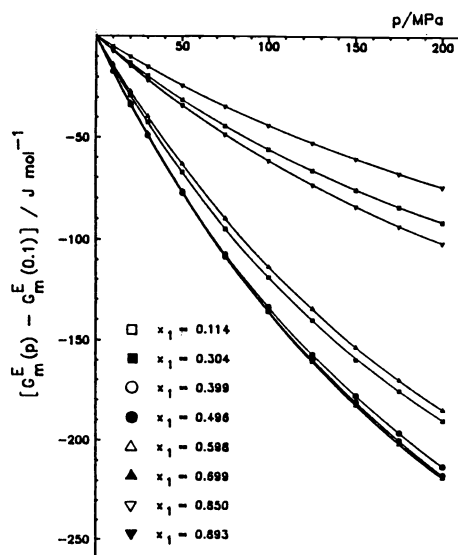


Fig. 3. $(G_m^E(p) - G_m^E(0.1 \text{ MPa})) / \text{J} \cdot \text{mol}^{-1}$ as a function of pressure for the system triethylamine(2) + chloroform (1) at 298.15 K (Kulka, refs 13, 14)

PHASE EQUILIBRIA OF POLAR FLUID MIXTURES AT HIGH PRESSURES

In the past the three different types of two-phase equilibrium in fluid mixtures - namely liquid-liquid, liquid-gas, and gas-gas equilibria - have normally been discussed separately. During the last two decades own systematic investigations, however, have shown that the limits between these three forms of heterogeneous phase equilibrium are not well defined and that continuous transitions occur. This hypothesis has been discussed in detail in the reviews mentioned above (refs 1-6) where also references are given. Thus there is no need to repeat these phase-theoretical arguments and the reader is referred to the literature cited.

In the following only some selected phase separation phenomena in binary as well as ternary systems at high pressures will be considered the accent being on solutions of alkanols (e.g. methanol, 1-hexanol, 1-decanol, 1-dodecanol) in liquid (e.g. alkanes) and supercritical (e.g. CO_2 , N_2 , CHF_3 , CClF_3) solvents and their mixtures. Most of these measurements have been performed in our laboratory during the last two or three years and are not yet published.

Our activities have been concentrated on these systems because solutions of alkanols in liquid and supercritical solvents are of increasing scientific and practical interest. They are model systems for the thermodynamic and statistical treatment and understanding of mixtures consisting of a polar, H-bonded component and a less polar or even unpolar solvent, and thus show interesting properties such as positive azeotropy and liquid-liquid immiscibility. In addition methanol and ethanol as well as their mixtures with hydrocarbons have practical importance as fuel substitutes and the higher normal alkanols are of interest for the pharmaceutical and food industries; e.g. fluid extraction of saturated and unsaturated fats, oils, waxes etc. and their derivatives from natural products might become a promising separation process on an industrial scale in addition to the decaffeination of coffee and the extraction of hops, spices etc. that are already in use.

Methanol + alkane systems

During the last two years liquid-liquid phase equilibria of several binary methanol + alkane systems have been investigated as a function of pressure up to 150 MPa in our laboratory, e.g. methanol + hexane (refs 22, 23), + heptane (ref.21), + octane (ref.21), + nonane (refs 22, 23), and + decane (refs 22, 23).

Very recently the systems methanol + butane and + pentane (ref.24) have also been studied. As a typical example selected results for methanol + pentane are presented in Fig.4 where some $p(T)$ curves for $x = \text{const}$ (so-called isopleths; Fig.4a) such as determined in the experiments and some $T(x)$ isobars (Fig.4b)

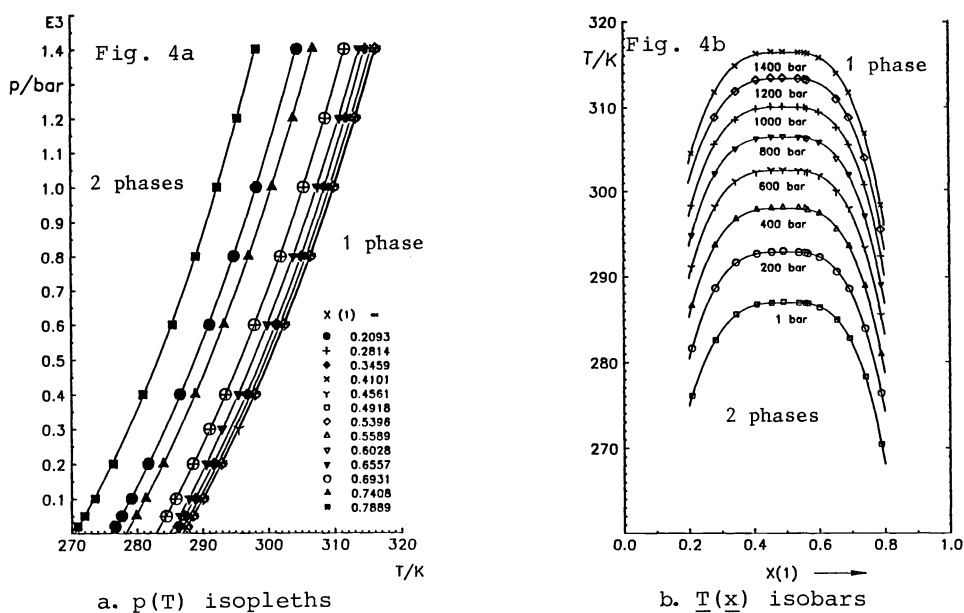


Fig. 4. Liquid-liquid equilibria in the system methanol(1) + pentane(2) (Haarhaus, ref.24)

that have been interpolated from the $\underline{p}(T)$ isopleths in Fig.4a are given. The results show that the system exhibits liquid-liquid immiscibility with upper critical solution temperatures that increase with increasing pressure. The $\underline{p}(T)$ isopleths could successfully be fitted to the Simon equation

$$\underline{T}/K = T_0 ((\underline{p}/\text{MPa})/a + 1)^{1/c} \quad (10)$$

and the $\underline{T}(x)$ isobars to the equation

$$\underline{T}/K = \underline{T}_0/K + k |\underline{y} - \underline{y}_c|^n \quad (11)$$

where

$$\underline{y} = \alpha \underline{x} / \{1 + \underline{x}(\alpha - 1)\} \quad (12)$$

$$\underline{y}_c = \alpha \underline{x}_c / \{1 + \underline{x}_c(\alpha - 1)\} \quad (13)$$

The correlations are discussed in detail in preceding papers (see e.g. refs 22, 23) where also numerical values of the parameters are given; it is interesting that from the fit $n > 3$ results. Equations (10) and (11) might also be promising for the correlation of other demixing systems at high pressures.

From the $\underline{p}(T)$ isopleths in Fig.4a the critical $\underline{p}(T)$ curve (which is the envelope of all isopleths) was determined. It is given in Fig.5 where the critical $\underline{p}(T)$ curves of all methanol + alkane systems studied in our laboratory are plotted and compared with some data on other systems taken from the literature. Whereas for methanol + methane (ref.25) the critical curve starts at the critical point (C.P.) of pure methanol and tends directly to higher pressures and lower temperatures, the critical $\underline{p}(T)$ curve of methanol + ethane (refs 26, 28) goes through a pressure maximum and minimum successively and then runs about vertically to higher pressures; thus methanol + ethane resembles a transition type to a gas-gas equilibrium system of the second kind (see refs 1-6). For all methanol + $n\text{-C}_n\text{H}_{2n+2}$ systems with $3 \leq n \leq 10$ the branches of the critical curves shown in Fig.5 correspond to liquid-liquid equilibria and end at so-called critical endpoints on the three-phase lines liquid-liquid-gas. It is an interesting fact that a negative initial slope of the critical curve is found for the system methanol + propane (refs 26, 27) whereas this slope is positive for the other systems. Besides a similar effect exists in alkane + CO_2 and + SF_6 systems (ref.29) and gives a hint for the existence of continuous transitions between liquid-liquid and gas-gas equilibria (refs 5, 29). From an extrapolation of the position of the critical $\underline{p}(T)$ curves in Fig.5 it has been recently deduced (ref.24) that in methanol + $n\text{-C}_n\text{H}_{2n+2}$ systems continuous critical $\underline{p}(T)$ curves and gas-gas equilibria of the second kind will again be found for about $n > 30$; experiments to check this extrapolation are underway.

Binary and ternary systems containing 1-dodecanol

In the investigations described in this section 1-dodecanol is used as a model substance to test different gases as supercritical solvents. The phase-theoretical aspects, however, will not be discussed here in detail (see refs 30, 31).

In Fig.6 $p(w)$ and $p(x)$ diagrams for binary 1-dodecanol + gas systems at 392 K (where w = mass fraction, x = mole fraction) are given (refs 30, 31). For 1-dodecanol + CO_2 (Fig.6a) the $p(w)$ and $p(x)$ curves correspond to a typical gas-liquid isotherm in the critical region, 1-dodecanol and CO_2 being completely miscible in all proportions at pressures above about 27 MPa. The phase behaviour of 1-dodecanol + CClF_3 is quite similar showing complete mutual miscibility at pressures that exceed about 35 MPa (Fig.6b). In the system 1-dodecanol + CHF_3 , however, no complete mutual miscibility is found (Fig.6c) and the mass and mole fractions of the alkanol pass through maximum values with increasing pressures respectively (curves on the left). Thus Fig.6 demonstrates that (comparing these three gases) CO_2 is the best and CHF_3 the poorest solvent for 1-dodecanol whereas CClF_3 is between them (see ref.33).

These findings suggest the use of CClF_3 , CHF_3 or another gas as a moderator for CO_2 . Such moderators play an important role in fluid extraction whenever the solvent power or the selectivity of a supercritical solvent (mostly CO_2) has to be changed. Systematic investigations with respect to these problems are underway in our laboratory (refs 30-33) some examples being given in Fig. 7. In Fig.7a and Fig.7b the moderator effect of CClF_3 and CHF_3 respectively on the solubility of 1-dodecanol in supercritical CO_2 is demonstrated by means of ternary phase diagrams for $T = \text{const} = 392$ K, the dashed lines being the ternary critical curves (refs 30, 31). The results are quite astonishing:

- Although CClF_3 is a much poorer solvent for 1-dodecanol than CO_2 the critical pressure of 1-dodecanol + CO_2 remains practically unchanged by the addition of CClF_3 up to rather high mass fractions of CClF_3 (Fig.7a).
- In spite of the fact that CHF_3 is a rather poor solvent for 1-dodecanol compared with CO_2 the critical pressure runs through a minimum, a maximum and again a minimum by the addition of CHF_3 (Fig.7b).

These findings give evidence that complicated molecular interactions will exist in solutions of this kind and demonstrate how difficult it is to understand and optimize moderator effects.

Another interesting critical phase behaviour in a related ternary system is shown in Fig.7c where the isothermal $p(x_1, x_2)$ phase diagram of the ternary system 1-dodecanol + hexadecane + CO_2 is given at $T = \text{const} = 393.15$ K (ref.32). Here the ternary critical curve runs through a distinct pressure minimum giving evidence for a typical cosolvency effect in this ternary mixture. Besides such a behaviour is rather often found in ternary systems where two binary miscibility gaps with similar critical pressures or temperatures exist (see e.g. ref.34).

Association of alkanols in supercritical solvents

Some years ago an analytical method was developed in our laboratory to measure the concentrations of selected components in high-pressure fluid phase separations without any sampling by near-infrared spectroscopy (NIR). The apparatus that has been described in detail elsewhere (refs 35, 36) has recently been used for the investigation of solutions of 1-hexanol and 1-decanol in supercritical CO_2 , CClF_3 and SF_6 at temperatures up to 400 K and pressures up to 70 MPa (ref.33). With the use of an integrated form of Lambert-Beer's law the total alkanol concentration was determined from the first overtone of the C-H stretching (1655 - 1790 nm) and the combination (2220 - 2370 nm) modes whereas the monomer concentration was obtained from the first overtone of the O-H stretching vibration, the difference of both corresponding to the concentration of associated alkanol species. Some selected results are presented in Fig.8 and 9.

Fig.8 shows four different $p(\log c)$ isotherms of the system 1-decanol + CO_2 at 343.4 K (Fig.8a), 362.9 K (Fig.8b), 382.5 K (Fig.8c) and 402.0 K (Fig. 8d) where c is the alkanol concentration in $\text{mg}\cdot\text{cm}^{-3}$. Here the total alkanol concentration (indicated by squares) as well as the concentrations of alkanol monomers (indicated by circles) or associated alkanol species (indicated by triangles) are plotted for the gaseous (three curves on the left) and the liquid (three curves on the right) phases, respectively. From Fig.8a-d the pressure and density dependence of these concentrations can be deduced. An important result is that in the gaseous phase most of the alkanol is monomeric at all

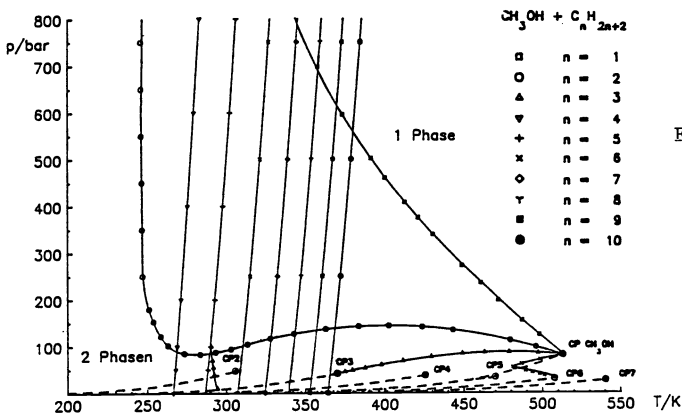
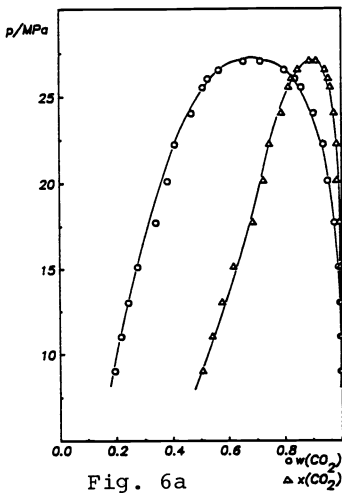
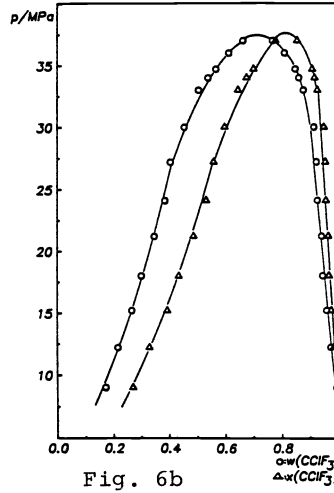


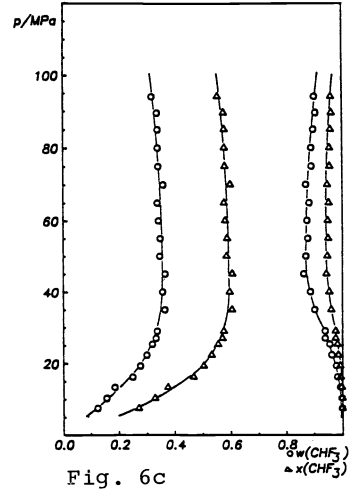
Fig. 5. Critical $p(T)$ curves of binary methanol + n -alkane systems (Haarhaus, ref. 24)



Dodecanol + carbon dioxide



Dodecanol + monochloro-trifluoromethane



Dodecanol + trifluoromethane

Fig. 6. $p(x)$ and $p(w)$ isotherms of binary fluid systems containing 1-dodecanol at 392 K (Katzenski, refs 30, 31)

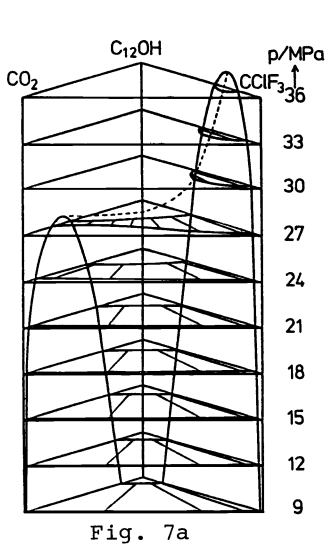


Fig. 7a

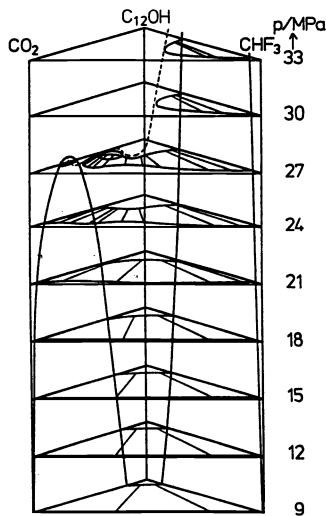


Fig. 7b

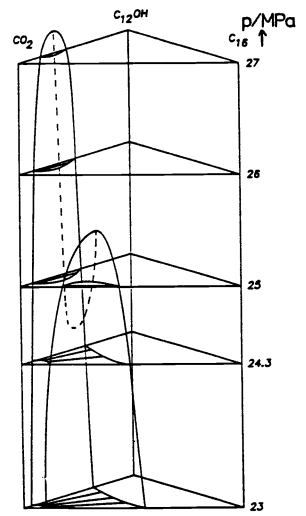


Fig. 7c

Fig. 7. Isothermal $p(\text{composition})$ diagrams of ternary 1-dodecanol systems
 a. 1-Dodecanol + CClF_3 + CO_2 at 392 K (Katzenski, refs 30, 31)
 b. 1-Dodecanol + CHF_3 + CO_2 at 392 K (Katzenski, refs 30, 31)
 c. 1-Dodecanol + hexadecanone + CO_2 at 393.15 K (Hölscher, ref. 32)

temperatures whereas in the liquid phase it is associated at low temperatures (see Fig.8a) but with increasing temperature the monomer concentration increases and finally exceeds that of the associates (see Fig.8d).

For the system 1-hexanol + CClF_3 (Fig.9) most of the alkanol is associated in both phases at the lowest measuring temperature (323.4 K, Fig.9a) but the concentration of monomers in the gaseous phase rapidly increases with increasing temperature and exceeds that of the associates at the highest temperature measured (401.8 K, Fig.9c). For a detailed discussion and additional data see ref.33.

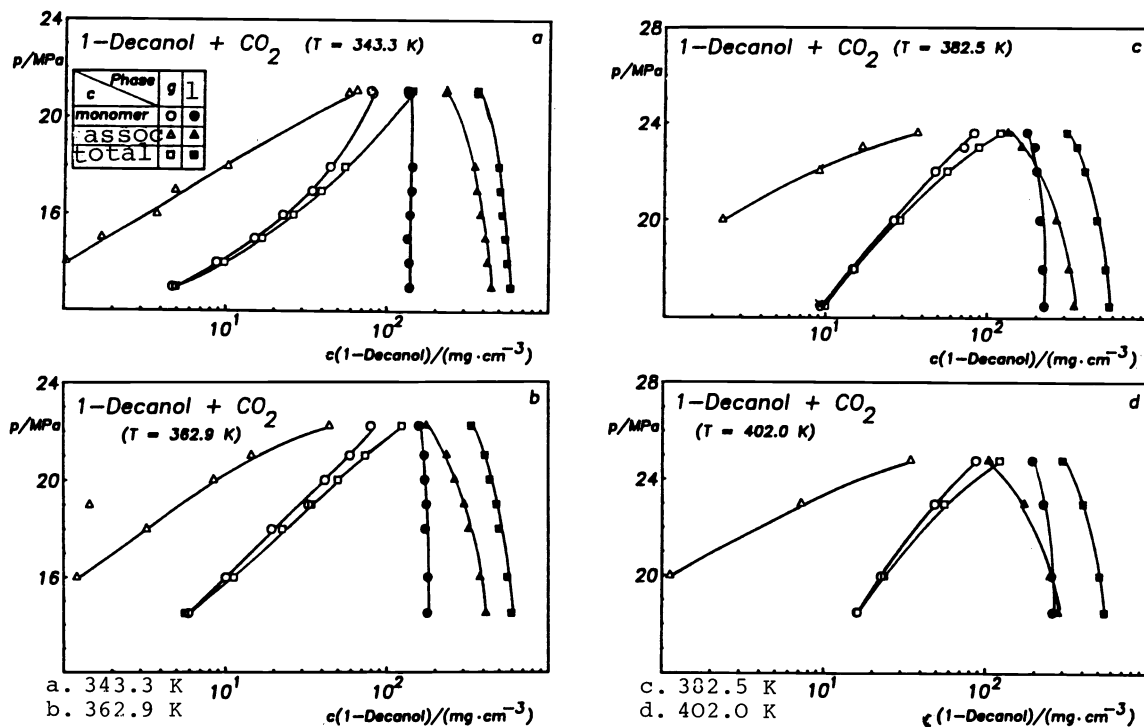


Fig. 8a - 8d. Isothermal $p(\log c)$ diagrams of the system 1-decanol + carbon dioxide: Total alkanol concentration, concentration of monomers, and concentration of associated alkanol (Nickel, ref. 33)

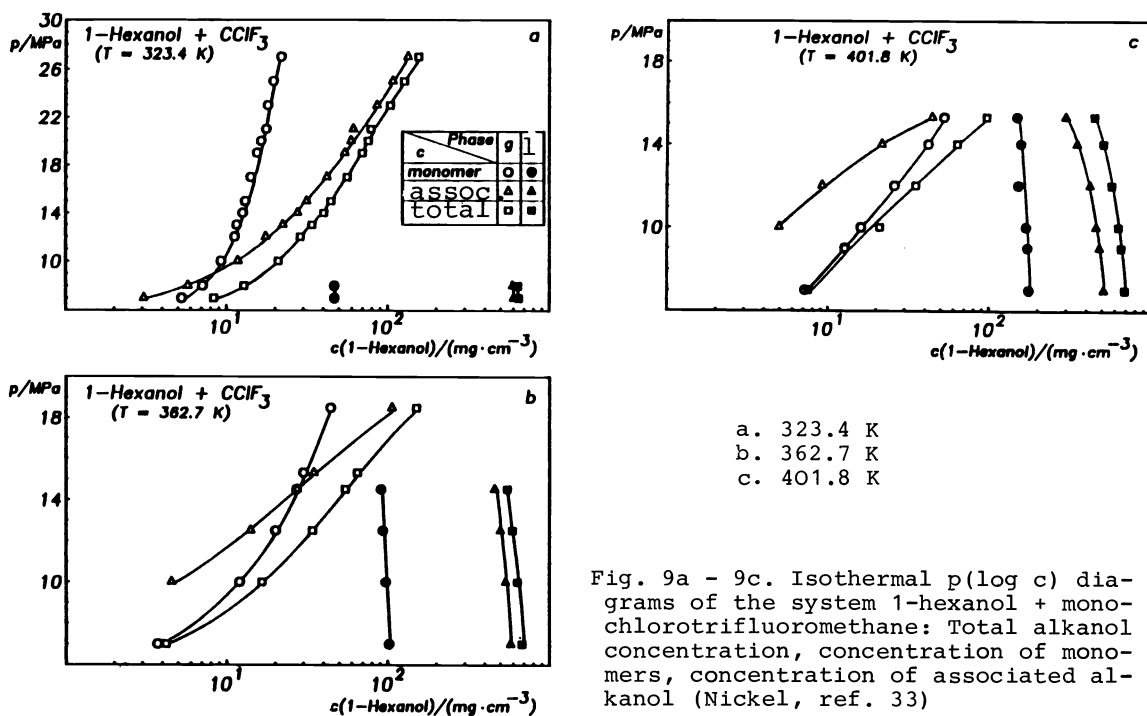


Fig. 9a - 9c. Isothermal $p(\log c)$ diagrams of the system 1-hexanol + monochlorotrifluoromethane: Total alkanol concentration, concentration of monomers, concentration of associated alkanol (Nickel, ref. 33)

Further investigations of this kind are underway (ref.37). They will be of considerable interest for the understanding of the solubility phenomena of alkanols in supercritical solvents as a function of temperature, pressure, density, dielectric constant etc. and from a molecular point of view as well as for the calculation and correlation of these phase equilibria taking into account the association of the alkanols.

Experimental

Experimental techniques and equipments are described in detail in the original literature (refs 21 - 24, 30 - 33, 35, 36). They are also reviewed in ref.7 where the equipments are given for the measurements on the methanol + alkane (ref.7, p.147) and the 1-dodecanol + gas (ref.7, p.152) systems as well as for the NIR experiments (ref.7, p.156); for additional informations and references see also ref.7.

Calculation and correlation of fluid phase equilibria

For the calculation and correlation of the phase equilibria and critical phenomena in fluid mixtures at high pressures mainly methods based on equations of state have been used in our laboratory; for a review with numerous references see Deiters (ref.38).

APPLICATIONS

Fluid mixtures, especially in the critical and supercritical region, are becoming increasingly interesting in many fields. Important applications are e.g. some new separation methods such as fluid extraction. Here decaffeination of coffee and extraction of hops with supercritical carbon dioxide are already used on an industrial scale. For an extensive discussion of these and other applications see e.g. refs 9 - 11, 39 - 42.

In supercritical fluid chromatography (SFC) compressed gases in the region of their critical temperatures are used as mobile phases. SFC is of interest for the separation or purification of low-volatile and thermolabile substances and for the determination of some physico-chemical properties (e.g. capacity ratios, diffusion coefficients) that are important for fluid extraction (refs. 43 - 49).

As an example some typical SFC chromatograms are shown in Fig.10 for the separation of a mixture of fat derivatives (1 = dodecyl phenyl ether, 2 = phenyl myristate, 3 = tetradecyl phenyl ether, 4 = phenyl palmitate, 5 = hexadecyl phenyl ether, 6 = phenyl stearate, 7 = octadecyl phenyl ether) with supercritical

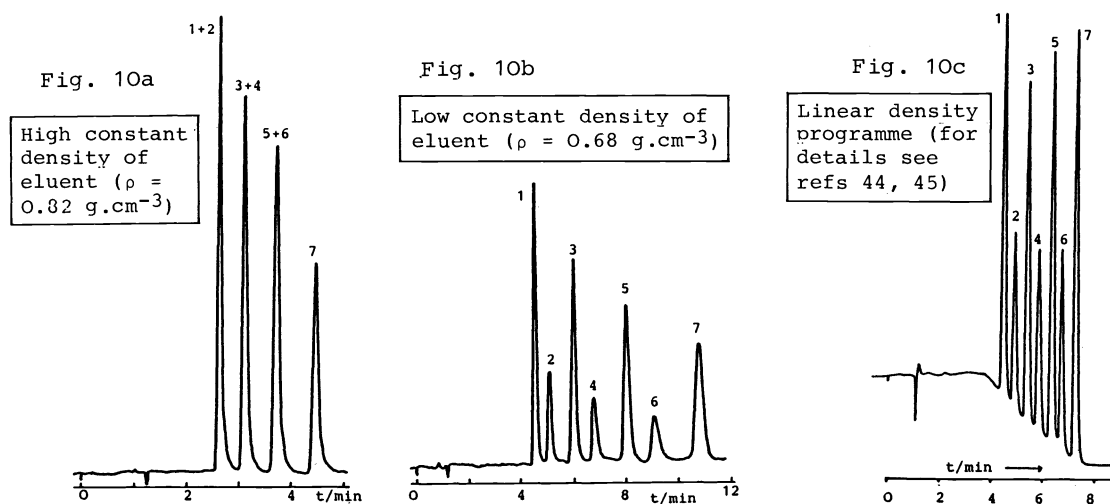


Fig. 10. SFC traces of a test mixture. Stationary phase: Spherisorb ODS 2. Mobile phase: CO₂, 39.5 °C. Mixture: 1 = dodecyl phenyl ether, 2 = phenyl myristate, 3 = tetradecyl phenyl ether, 4 = phenyl palmitate, 5 = hexadecyl phenyl ether, 6 = phenyl stearate, 7 = octadecyl phenyl ether (Wilsch, refs 44, 45)

carbon dioxide by means of isothermal - isobaric (Fig.10a, 10b) and isothermal - density programmed (Fig.10c) supercritical fluid chromatography (refs 44, 45). At high density of the mobile phase the separation is incomplete (Fig.10a), at lower density it is complete but more time-consuming (Fig.10b). Thus Fig.10a and Fig.10b give evidence for the fact that with decreasing pressure the selectivity of carbon dioxide as a supercritical solvent increases whereas the solvent power decreases. With the density program, however, a good and rapid separation is obtained (Fig.10c).

From the isothermal - isobaric experiments capacity ratios k were calculated according to

$$\underline{k} = \frac{c_{\text{stat}}}{c_{\text{mob}}} \cdot \frac{v_{\text{stat}}}{v_{\text{mob}}} = \frac{t_R - t_0}{t_0} \quad (14)$$

where c_{stat} and c_{mob} are the concentrations of the sample and v_{stat} and v_{mob} the volumes of the stationary and mobile phases respectively and t_R the retention time of the substance under test and t_0 the retention time of a non-retained compound respectively. According to Eq (14) the capacity ratio k is proportional to the distribution coefficient $\underline{K} \equiv c_{\text{stat}}/c_{\text{mob}}$ and, since $v_{\text{stat}}/v_{\text{mob}}$ is about constant, k as a function of pressure is a measure of the pressure dependence of \underline{K} . Thus \underline{k} is a highly interesting thermodynamic parameter.

In Fig.11 k is plotted on a logarithmic scale versus density ρ for all components of the mixture separated in Fig.10 (ref. 44). Fig.11 demonstrates that all k decrease by more than one order of magnitude when increasing the density from about 0.5 to 0.8 g·cm⁻³. In addition Fig.11 illustrates why a better separation of the mixture is found at lower densities since some of the log $k(\rho)$ isotherms intersect at high densities.

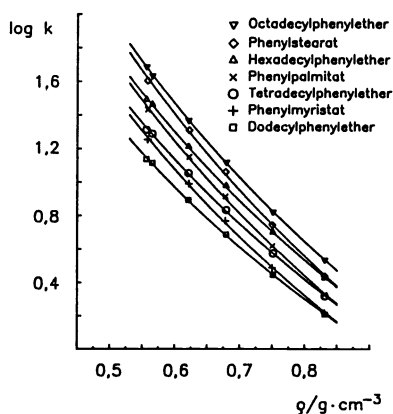


Fig. 11. Log $k(\rho)$ isotherms of the components of the same test mixture as in Fig. 10. Stationary phase: Spherisorb ODS 2. Mobile phase: CO₂, 39.5 °C (Wilsch, ref. 44)

For the determination of binary diffusion coefficients D_{12} the usual separation column is replaced by an empty capillary tube of suitable length and diameter. With some assumptions the following simplified equation results from the mathematical treatment

$$\underline{H} = \frac{2 D_{12}}{\bar{u}} + \frac{r_0^2 \bar{u}}{24 D_{12}} \quad (15)$$

$$\underline{H} = \frac{\sigma^2(x)}{\bar{u}} \quad (16)$$

where $\sigma^2(x)$ is the peak variance expressed as a length, \bar{u} the average velocity of the mobile phase, r_0 the inner radius and \underline{l} the length of the capillary tube.

In Fig.12a D_{12} data for 1,4-dimethylbenzene in SF₆ are given as a function of pressure p for some different temperatures (refs 47 - 49). D_{12} values up to 2·10⁸ m²·s⁻¹ are obtained at the highest temperatures and the pressure dependence reaches a maximum value in the vicinity of the critical point of SF₆. With decreasing temperatures D_{12} also decreases and becomes less pressure dependent, as it is the normal case for liquids far away from their critical

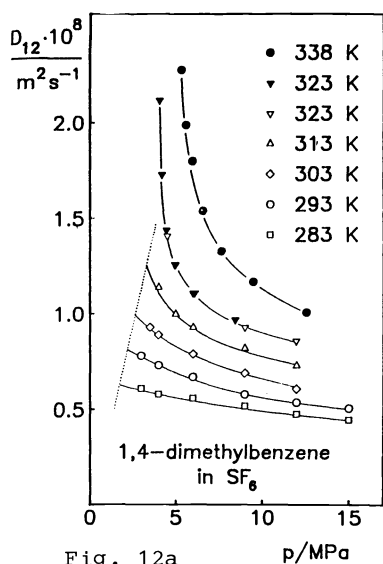


Fig. 12a

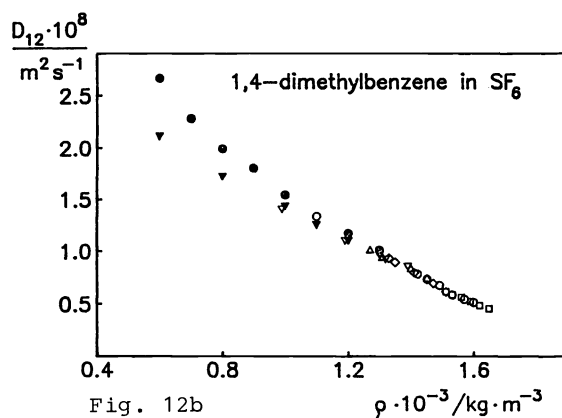


Fig. 12b

\underline{D}_{12} as a function of density ρ

\underline{D}_{12} as a function of pressure p

Fig. 12. Binary diffusion coefficients \underline{D}_{12} for 1,4-dimethylbenzene in SF_6 at six different temperatures (Kopner, ref.47, Ellert, ref. 48, ref. 49)

points. In Fig.12b the same data as in Fig.12a are plotted versus the density ρ of SF_6 instead of versus pressure p . It is remarkable that for densities of about $1.3 \text{ g}\cdot\text{cm}^{-3}$ there is little if any influence of temperature, \underline{D}_{12} being determined by the density of the system only. Thus Fig.12b makes evident that the 'pressure dependence' of \underline{D}_{12} is predominantly a result of density changes. For a more detailed discussion see refs 47 - 49.

CONCLUSION

The present review demonstrates that some interesting effects can be observed in fluid mixtures at high pressures. Here a most important advantage is the possibility to study physico-chemical phenomena as a function of density and even at constant densities where the intermolecular distances also remain essentially constant. Owing to rapid developments in experimental high-pressure techniques, the ranges of temperatures and pressures involved are already accessible quite easily and at moderate costs.

Acknowledgement

Financial support of the Deutsche Forschungsgemeinschaft (DFG), the Minister für Wissenschaft und Forschung des Landes Nordrhein-Westfalen and the Fonds der Chemischen Industrie e.V. are gratefully acknowledged.

REFERENCES

1. G.M. Schneider, *Ber. Bunsenges. Phys. Chem.* **70**, 497 - 520 (1966).
2. G.M. Schneider, *Pure & Appl. Chem.* **47**, 277-291 (1976).
3. G.M. Schneider, in *Chemical Thermodynamics*, Vol. 2, M.L. McGlashan ed., A Specialist Periodical Report, London, 1978, Chap. 4, p. 105 - 146.
4. G.M. Schneider, *Pure & Appl. Chem.* **55**, 479 - 492 (1983).
5. G.M. Schneider, *Ber. Bunsenges. Phys. Chem.* **83**, 841 - 848 (1984).
6. G.M. Schneider, *Thermochimica Acta* **88**, 17 - 34 (1985).
7. U.K. Deiters and G.M. Schneider, *Fluid Phase Equil.* **29**, 145 - 160 (1986).
8. G.M. Schneider, M. Dittmann, U. Metz, and J. Wenzel, *Pure & Appl. Chem.* **59**, 79 - 90 (1987).
9. G.M. Schneider, E. Stahl, and G. Wilke eds., *Extraction with Supercritical Gases*, Verlag Chemie, Weinheim 1980.
10. M.E. Paulaitis, J.M.L. Penninger, R.D. Gray, Jr., and P. Davidson, *Chemical Engineering at Supercritical Fluid Conditions*, Ann Arbor Science Publishers, Michigan 1983.

11. E. Stahl, K.W. Quirin, and D. Gerard, *Verdichtete Gase zur Extraktion und Raffination*, Springer Verlag, Berlin, Heidelberg, New York, Paris, Tokio 1987.
12. G. Götze, Doctoral Thesis, University of Bochum, 1976.
13. J. Kulka, Diploma Thesis, University of Bochum, 1986.
14. J. Kulka and G.M. Schneider, *J. Chem. Thermodynamics* **19**, 205 - 214 (1987).
15. J. Rübesamen, Diploma Thesis, University of Bochum, 1987.
16. J. Rübesamen and G.M. Schneider, *J. Chem. Thermodynamics*, in press.
17. L.G. Hepler and D.V. Fenby, *J. Chem. Thermodynamics* **5**, 471 - 475 (1973).
18. D.V. Fenby, A. Chand, A. Inglese, J.-P.E. Grolier and H.V. Kehiaian, *Aust. J. Chem.* **30**, 1401 - 1410 (1977).
19. J.J. Christensen, T.A.C. Walker, D.R. Cordray, and R.M. Izatt, *J. Chem. Thermodynamics* **19**, 47 - 56 (1987).
20. A. Kohl and A. Heintz, *Thermochimica Acta* **94**, 79 - 84 (1985).
21. J.B. Ott, I.F. Hölscher, and G.M. Schneider, *J. Chem. Thermodynamics* **18**, 815 - 826 (1986).
22. I.F. Hölscher, Diploma Thesis, University of Bochum, 1986.
23. I.F. Hölscher, G.M. Schneider, and J.B. Ott, *Fluid Phase Equil.* **27**, 153 - 169 (1986).
24. U. Haarhaus, Diploma Thesis, University of Bochum, 1986.
25. E. Brunner, *J. Chem. Thermodynamics* **17**, 671 - 679 (1985).
26. E. Brunner, *J. Chem. Thermodynamics* **17**, 871 - 885 (1985)
27. J.P. Kuenen, *Phil. Mag., Serie 6*, **6**, 637 (1903).
28. Z. Alwani and G.M. Schneider, *Ber. Bunsenges. Phys. Chem.* **80**, 1310 - 1315 (1976).
29. I. Matzik and G.M. Schneider, *Ber. Bunsenges. Phys. Chem.* **89**, 551 - 555 (1985).
30. G. Katzenski-Ohling, Doctoral Thesis, University of Bochum, 1986.
31. G. Katzenski-Ohling and G.M. Schneider, *Fluid Phase Equil.*, in press.
32. I.F. Hölscher, Doctoral Thesis, University of Bochum, in preparation.
33. D. Nickel, Doctoral Thesis, University of Bochum, 1987.
34. R. Paas, K.H. Peter, and G.M. Schneider, *J. Chem. Thermodynamics* **8**, 741 - 747 (1976).
35. I. Swaid, Doctoral Thesis, University of Bochum, 1984.
36. I. Swaid, D. Nickel, and G.M. Schneider, *Fluid Phase Equil.* **21**, 95 - 112 (1985).
37. J. Friedrich, Doctoral Thesis, University of Bochum, in preparation.
38. U.K. Deiters, in ACS Symposium Series No. 300, *Equations of State: Theories and Applications*, K.C. Chao and R.L. Robinson, Jr., eds, American Chemical Society 1986; p. 371 - 388.
39. *Sep. Sci. Techn.* **17**(1), 1 - 287 (1982).
40. *Fluid Phase Equil.* **10**(2-3), 135 - 358 (1983).
41. G. Brunner and S. Peter, *Chem.-Ing.-Techn.* **53**, 529 - 542 (1981).
42. D.F. Williams, *Chem. Eng. Sci.* **36**, 1769 - 1788 (1981).
43. U. van Wasen, I. Swaid and G.M. Schneider, *Angew. Chem. Int. Ed. Engl.* **19**, 575 - 587 (1980).
44. A. Wilsch, Doctoral Thesis, University of Bochum, 1985.
45. A. Wilsch and G.M. Schneider, *J. Chromatogr.* **357**, 239 - 252 (1986).
46. K.H. Linnemann, A. Wilsch, and G.M. Schneider, *J. Chromatogr.* **369**, 39 - 48 (1986).
47. A. Kopner, Diploma Thesis, University of Bochum, 1984.
48. J. Ellert, Diploma Thesis, University of Bochum, 1986.
49. A. Kopner, A. Hamm, J. Ellert, R. Feist, and G.M. Schneider, *Chem. Eng. Sci.*, in press.